

Keywords

Heat Flow,
Beiras Region, Portugal
Radioactive heat sources,
Lithosphere thickness,
Curie temperature depth,
Mantle heat flow.

Received: January 30, 2020

Accepted: February 24, 2020

Published: April 01, 2020

Numerical Simulations of Terrestrial Heat Flow in the Beiras Region, Mainland Portugal

Maria Rosa Duque ¹

¹ Departamento de Física/Escola de Ciências e Tecnologia, Universidade de Évora, Évora, Portugal.

Email address

mrada@uevora.pt (M.R. Duque)

Corresponding author

Abstract

Numerical simulations of heat flow density have been made for ten localities in the Beiras region of central Portugal where observational data are absent. The procedure adopted is based on results of deep crustal geophysical surveys and consider that the heat flow measured at the surface of the Earth results from the addition of heat generated in the crust by radioactive sources to that coming from the mantle. Radioactive heat sources in the region are heterogeneous and heat flow values at the surface depends on the thickness of upper crustal layers. Geotherms were obtained considering heat flow by conduction in the vertical direction. The models employed make use of data derived from geophysical surveys of Moho depths and detailed results related with seismic velocity distribution in the crust. In addition, results of radiometric surveys were employed in deriving heat production values for upper layers of the crust. A value around 35 mW m^{-2} was assumed for heat flow from the mantle. The resulting heat flow density values are similar to those found for areas with similar tectonic characteristics in NW Africa and in Southern Portugal.

1. Introduction

Results of deep crustal geophysical surveys usually provide the basis for understanding the framework of tectonic interactions occurring in near surface layers of the Earth. However, a major problem in study of associated crustal thermal regime is the low data density of heat flow in areas of geophysical surveys. For obvious practical reasons few deep heat flow measurements are carried out in localities along profiles of geophysical surveys. A convenient solution to this problem is numerical simulations of heat flow values that are compatible with crustal structure and results of deep geophysical surveys. This approach was adopted in the present work, where we consider that reasonable estimates of surface heat flow can be obtained based on geoid anomalies and crustal radiometric data.

Our study was made in parts of Beiras Region located in Central Portugal, near the Spanish border, along the Western part of the Iberian Peninsula. It is located between latitudes 39.8°N and 41.0°N and longitudes 6.8°W and 7.7°W . No heat flow measurements have been reported for this region. However, according to the Heat Flow Density Map of the Atlas of Geothermal Resources of Europe (2002) estimated heat flow values fall in the range of 50 and 60 mW m^{-2} .

The map of Figure 1 illustrates the general geological characteristics of northern Portugal in which the green rectangle indicates the location of the study area.

Lamas et al (2017) reported abundances of Uranium, Thorium and Potassium in rocks representative of local geologic formations. These results have allowed determination of crustal heat production by decay of radioactive elements in the region. The locations of our study were chosen outside the fault regions to avoid perturbations in the heat conduction process.

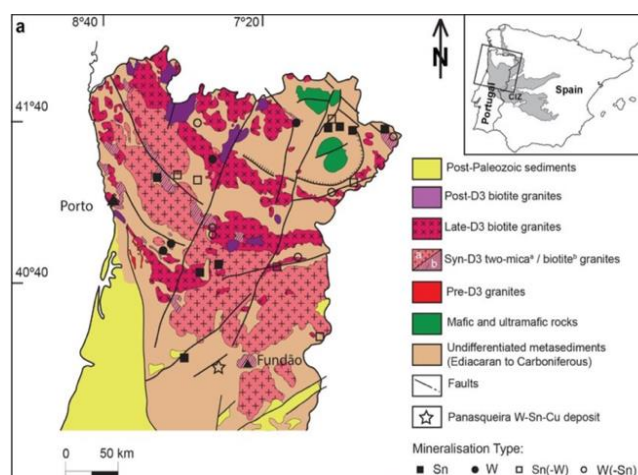


Figure 1 - Map illustrating the general geological characteristics of the Beiras region in northern Portugal (Codeco et al, 2017). The green rectangle indicates the location of the study area.

2. Geologic Context

Geologically speaking the main type of formations that outcrop at the surface in the region are granitic rocks surrounded by schists. Granites of three different ages with different contents of Uranium Thorium and Potassium appearing in formations of different thicknesses were identified in the region (Lamas et al, 2015; Veludo et al, 2017). Several faults traverse the region that has been subjected to intra plate deformation (De Vicente et al, 2018) since the Miocene originating several blocks in the crust with different Moho depth values (Dundar et al ,2016; Diaz et al, 2016) and different altitude values of the surface.

Crustal thickness values considered here are coincident with Moho depth values obtained from seismic data (Dundar et al, 2016; Mancilla et al (2015); Diaz et al, 2016). The region is crossed by several faults. Two main active faults can be identified in the region. The Manteigas-Vilariça- Bragança fault located near the western border of the region on study, generated in Late-Variscan time and reactivated by Alpine compression during the Cenozoic (Cabral,1995 ; Cabral et al, 2010; Rockwell et al, 2009) and the Ponsul fault located in the SE of the region affecting basement rocks of the Centro Iberian Zone (Cabral, 2019).

3. Methodology and Data Sets Employed

In the absence of tectono-thermal processes, it is reasonable to argue that heat flow measured at the surface (Q_0) include contributions from crustal heat sources (Q_c) as well as deep heat flow from the mantle (Q_M). Thus, Q_0 is sum of crustal and mantle heat flux components:

$$Q_0 = Q_c + Q_M \quad (1)$$

It is further argued that estimates of mantle heat flow compatible with results of seismic surveys and determinations of geoid anomalies coupled with values of radioactive heat sources derived from crustal radiometric surveys provide reasonable constraints on heat flow at the surface. This is the essence of the approach adopted in the present work.

The different layers of the crust and its thickness values were obtained from models of the region made with seismic data (Veludo et al, 2017). In addition to vertical profiles of seismic velocity distribution in the region, horizontal distributions of seismic velocities at different depths are also considered. Information from vertical profiles BB', GG' and HH' as horizontal distribution of seismic velocities at different depths were selected for the present work.

The ten points studied are located inside the region delimited by the blue rectangle in the map of figure 2. Table 1 provides information on geographic coordinates and altitudes of the ten locations considered in the present work. Geotherms were obtained using the heat flow density values and considering steady- state heat conduction in the vertical direction (Duque, M.R., 2018). A value of 15°C was used as 3temperature in the upper boundary of the model (temperature at the surface). Thermal conductivity data used for the lower crust was 2.1 WK⁻¹ m⁻¹ and for the upper crust 2.5 WK⁻¹ m⁻¹. In the upper layers of the crust thermal conductivity values measured in the region were used considering the geological formation of the point considered and the thermal conductivity

values obtained in measurements on samples collected in mainland Portugal.

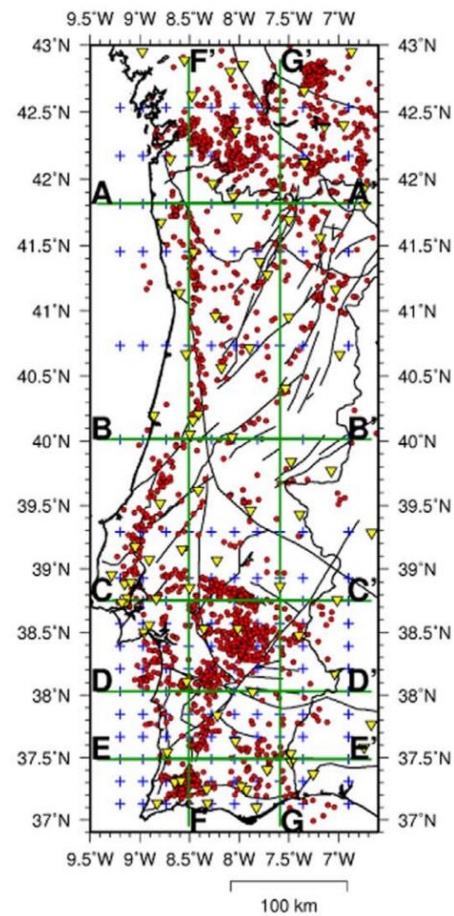


Figure 2 - Locations of seismic profiles (adapted from Veludo et al, 2017) and the region on study (blue rectangle). The red dots indicate epicenters of crustal seismic events.

Table 1 - Point location and altitude values used.

Point number	Latitude N	Longitude W	Altitude (m)
1	40.93	7.64	850
2	40.60	7.64	660
3	40.47	6.98	770
4	40.79	7.19	500
5	40.65	7.38	450
6	39.89	6.97	350
7	40.20	7.19	650
8	40.00	7.50	450
9	40.45	7.28	700
10	40.37	7.42	800

Heat production by decay of radioactive elements in the upper layers of the crust was obtained from Uranium, Thorium and Potassium content in the rocks (Lamas et al, 2015; Lamas et al, 2017) and natural gamma-ray charts (LNEG, 2013; IGM, 1997) in the region (Duque, 2018b). A constant value of 0.1 μW m⁻³ was used for heat production in the lower crust. No heat production was considered in the upper mantle. Values close to 35 mW m⁻² were used for heat flowing from the mantle. The values obtained for the heat flow at the surface Q_0 , the heat generated in the crust Q_c and the heat flowing from the mantle Q_M , are presented in Table 2.

Table 2 - Heat flow density data at the surface Q_o , heat flow originated in the crust Q_c and heat flowing from the mantle Q_M .

Point number	Q_o (mWm ²)	Q_c (mWm ²)	Q_c/Q_M
1	81	46	0.57
2	90	56	0.61
3	94	59	0.63
4	89	54	0.61
5	90	55	0.61
6	90	55	0.61
7	81	46	0.57
8	91	56	0.62
9	99	64	0.65
10	87	52	0.60

In this table, the maximum value of surface heat flow (Q_o) is 99 mW m⁻² while the heat flowing from the mantle (Q_M) has a value of approximately 35 mW m⁻². Thus, heat generated in the crust (Q_c) comprise a fraction of 0.646 of Q_o . Temperature value at Moho depth is 630°C. The layer between 21 and 22km makes the transition from the middle to the lower crust. The first layer of the model is formed by granites with high heat production values.

Note that heat flow density values fall in the interval of 81 and 99 mW m⁻². This does not necessarily mean that heat flow density values lower than 81 mW m⁻² or higher than 99 mW m⁻² cannot exist in the region. The values obtained depend on heat production by radioactive sources of the crust and thickness of the layers where they are located. The highest heat production value used in the present work is 5 μW m⁻³ but values of 5.51 ± 1.34 μW m⁻³ were obtained in laboratory measurements (Miranda et al, 2015) using samples collected in the region. It is not possible to identify in the Gamma Ray Chart (LNEG, 2013; IGM,1997) the anomalous region associated with this value and it was concluded that the thickness and surface area of the formation would possible be too small to be detected in the chart.

4. Results and discussion

The thermal conductivity values adopted for the crustal layers at this site fall in the interval of 3.4 to 2.1 W/m/K, with larger values for upper crustal layers. Heat production values also follow a similar trend. The heat flow values found are similar to values occurring in other regions like NW Africa, South of Portugal and some regions in Spain (Rimi et al, 2005; Duque and Mendes Victor, 1993; Pollett et al, 2019). The heat flow value from the mantle was obtained from measured values in neighboring regions and the geoid height values obtained in the region, not explained by world gravity data maps (Bonvalot et al, 2012).

Table 3 presents thermal conductivity and heat production values used and depth intervals considered in the study of site described as point 9. Five different depth intervals were considered. Negative depths indicate locations above mean sea level.

Tables 4 presents data obtained from geotherms and crustal thickness used in the different models. A temperature interval of 17°C is obtained at 1 Km depth. Temperature values at this depth are influenced by altitude values of the surface (the point with the lowest temperature value (Point 6) has an altitude of 350 m (above sea level) and the point with the highest value (Point 3) has an altitude of 770 m (above sea level). A

temperature interval of 36°C was obtained at 10 Km depth. This value gives information about the heterogeneity of the region and the heat flow density values used. At 25 Km depth (lower crust) the temperature interval is 25°C. The temperature interval decreases with the increase in depth. At 90 Km depth its value is 7°C. We must remember that geotherms were made with models of heat conduction in the vertical direction. With two-dimensional model values of heat flow in the horizontal direction will appear and this value will tend to decrease.

Table 3 - Parameter values used in the study of site described as point 9.

Depth interval (Km)	Thermal conductivity (W K ⁻¹ m ⁻¹)	Heat production (μ W m ⁻³)
-0.7 – 3.5	3.4	5
3.5 – 12.0	3.15	2.7
12.0 - 21.0	2.5	2.0
21.0 - 22.0	2.3	1.23
22.0 - 29.0	2.1	0.1

Table 4 - Temperatures in Celsius degrees obtained for different depth levels (values referred to mean sea level).

Point number	Temperatures (°C)			
	1 km	5 km	10 km	25 km
1	59	143	256	529
2	57	145	263	537
3	64	166	278	539
4	56	154	260	534
5	52	149	262	536
6	47	133	242	514
7	55	147	249	519
8	54	156	262	529
9	62	160	264	533
10	57	154	262	531

Table 5 presents values deduced from geotherms and crustal thicknesses used in the different models. Ten models of the crust were considered and temperature values versus depth (geotherms) were obtained. In this table the depth values considered for Curie temperature (CPD values) is 570°C while the basal temperature of the lithosphere with thickness (LT) is 1350° C.

The percentage of heat generated in the crust varies from 57 to 65% of the heat flow values obtained at the surface. The lower values appear associated with schist formations (point 7 and point 10) where the content of radioactive elements is lower than in granites (1.93 and 1.9 μW m⁻³ respectively). Point 1 is located in a granite formation but with a low value of upper crust thickness. The highest values (point 3 and point 9) are associated to granites with heat production values of 3.42 and 5 μW m⁻³ respectively.

Curie Temperature depth values are located in the interval from 27 Km to 29 Km. The highest values were obtained in point 6 and point 7, located in schist formations and in regions with higher crustal thickness values (31 Km). All CPD values are located in the lower crust and are higher than values obtained for the same region in studies using different methodologies (André et al, 2018). Lithosphere thickness values of 96 Km were obtained. These values are similar to the values found in the South of Portugal (Duque, 2018a).

Table 5 - Data obtained from geotherms and crustal thickness used.

Point number	CPD (km)	LT (km)	CT (km)
1	28	96	30
2	28	96	30
3	28	96	30
4	28	96	29
5	27	96	29
6	29	96	31
7	29	96	31
8	28	96	31
9	28	96	30
10	28	96	30

Due to intra plate stress affecting the region (De Vicente, 2018) vertical movements of the different blocks have occurred. Using geoid heights obtained in 2008 and 1996 (Online geoid calculator-Source Forge) it is possible to obtain geoid height variation during the time interval mentioned. The beginning of this movement is not known and a time interval for its occurrence is not predictable. Due to the time interval associated with conductive processes direct relations using altitudes of the different points were not used.

Figure 3 shows the relation between heat flow density values at the surface and geoid heights in 2008. Heat flow densities around 90 mW m^{-2} were found in places with geoid heights from 55.23 m to 56.35 m. Point 6 and point 8 (grey points) are located near the southern border of our region of study presenting lowest latitude values of the points studied. A linear trend seems to exist with values from points 7,4,2,5,3 and 9 (orange points), suggesting a relation between heat generated in the crust and geoid height.

We must say also that geoid values are higher than 55 m and lower than 57 m. This means that we are working with very high values of geoid height presenting alterations in low periods of time and the value increase in some points but decrease in other points. Figure 4 shows the relation between Geoid heights and differences between geoid heights obtained in years 2008 and 1996.

Four different groups of values and one isolated point can be seen in Figure 4. No clear relation between geoid variations and heat flow values was detected. The values obtained show clearly that the blue point in the graph, with the highest value of geoid height (point 1) shows a variation of $+ 0.7341 \text{ m}$. Points 6 and 8 presenting lowest geoid height values, located in the lowest latitudes (39.89 and 40.00 N) show identical variation in geoid height. Yellow points (point 9 and 10) show identical variations but with a higher value than points 6 and 8. Points 2 and 5 (orange points) shows the lowest variations in the group but in point 2 Geoid height is decreasing and in point 5 it is increasing. This fact suggest that mechanical aspects must be studied together with the thermal problem. This study is outside the scope of this work.

5. Conclusions

Heat flow density values located between 81 and 99 mW m^{-2} were obtained for ten points located in the region using seismic velocities distributions reported by Veludo et al (2017) in the region studied.

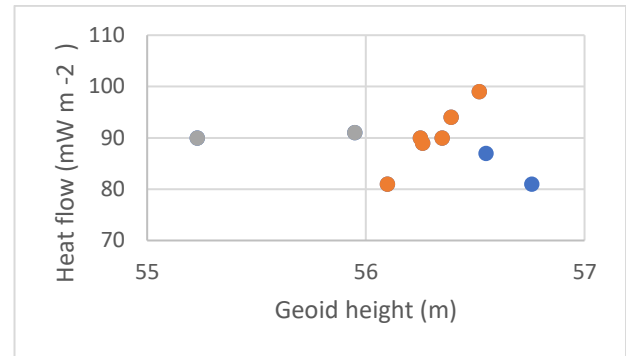


Figure 3 - Relation between heat flow versus Geoid height at sites of the ten points considered in the present work.

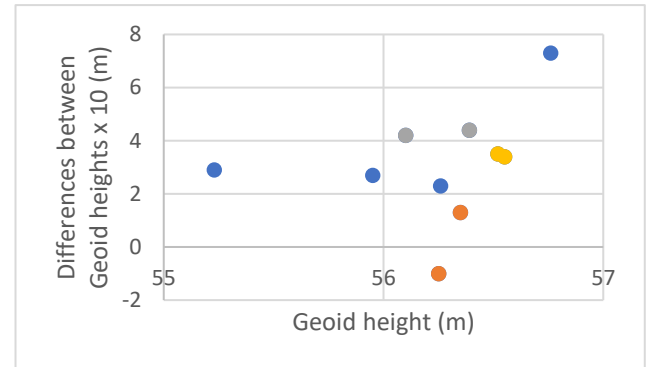


Figure 4 - Relation between Geoid height versus Geoid height variations ($\times 10^2$) at sites of the ten points considered in the present work.

Curie temperature (570°C) depth values of from 27 to 29 km were found considering heat flow by conduction in the vertical direction. Temperature values of 1350°C (considered as representative of the thermal field at the bottom of the lithosphere) were found to occur at depths of 96 km.

The upper and middle crust in the region in the study area very heterogeneous. Consequently, the difference between the heat flow density values arise is mainly from variations in radioactivity heat sources and thicknesses of the upper layers of the crust. The surface heat production values are compatible with laboratory measurements reported by Miranda et al (2015) using samples collected in the region.

Due to the heterogeneity of the crust and the different values of the heat sources two and /or three-dimensional studies are needed to obtain a better understanding of the heat flow distribution in the region.

6. Acknowledgments

This study was carried as part of research work at the University of Evora, Portugal.

This work benefited from suggestions and modifications made by the editorial staff of IJTHFA.

References

- André, J., Marzán, I., Ayarza, P., Linares, D., Palomeras, I., Torné, M., Campbell, S., Carbonell, R., 2018. Curie Point Depth of the Iberian Peninsula and surrounding Margins. A Thermal and Tectonic Perspective of its Evolution. *J. Geophys. Res.*,123 (3), 2049-2068, <https://doi.org/10.1002/2017JB014994>.

- Bonvalot, S., Briais, A., Peyrefitte, A., Gabalda, G., Balmino, G., Moreaux, G., 2012. World Gravity Map/ Carte gravimétrique Mondiale, Bureau Gravimétrique International (BGI), Paris, France. www.ccgm.org.
- Cabral, J., 1995. Neotectonics of Mainland Portugal (in Portuguese) Memórias do Instituto Geológico e Mineiro, 31, Lisboa.
- Cabral, J., Perea, H., Figueiredo, P.M., Besana-Ostman, G., Brum da Silveira, A., Cunha, P.P., Gomes, A., Lopes, F.C., Pereira, D., Rockwell, T., 2010. Preliminary results of a paleo seismological study of the Vilariça fault (NE Portugal). In: J. M. Insua, F. Martín González (eds), Contribution da la Geologia al análisis de la Peligrosidad Sísmica, Livro de Resumos da 1ª Reunião Ibérica sobre Falhas Activas e Paleossismologia, 41-44.
- Cabral, J., 2012. Neotectonics of mainland Portugal: state of the art and future perspectives. *Journal of Iberian Geology*, 1, 71-84.
- Cabral, J., 2019. Active Faults in Mainland Portugal (West Iberia). In: C. Quesada, J. T. Oliveira (eds), *The Geology of Iberia: A Geodynamic Approach*, Regional Geology Reviews, Springer Nature Switzerland AC 2019. DOI:10.1007/978-3-030-10931-8_4
- Codeço, M.S., Weis, P., Trumbull, R., Pinto, F., Lecumberri-Sanchez, P., Wilke, F.D.H., 2017. Chemical and boron isotopic composition of hydrothermal tourmaline from the Panasqueira W-Sn-Cu deposit, Portugal. *Chemical Geology*. 10.1016/j.chemgeo.2017.07.011.
- De Vicente, G., Cunha, P.P., Muñoz-Martín, A., Cloetingh, S., Olaiz A., Vegas, R., 2018. The Spanish-Portuguese Central System: An Example of Intense Intraplate Deformation and Strain Partitioning. *Tectonics*, 37, 4444-4469. DOI 10.1029/2018TC005204.
- Dias, G., Leterrier, J., Mendes, A., Simões, P. & Bertrand, J., 1998. U-Pb zircon and monazite geochronology of post-collisional Hercynian granitoids from the Central Iberian Zone (Northern Portugal). *Lithos*, 45, 349-369.
- Diaz, J., Gallart, J., Carbonell, R., 2016. Moho topography beneath the Iberian-Western Mediterranean region mapped from controlled-source and natural seismicity surveys, *Tectonophysics*, 692, 74-85.
- Dundar, S., Dias, N.A., Silveira, G., Kind, R., Vinnik, L., Matias, L., Bianchi, M., 2016. Estimation of crustal Bulk properties beneath Mainland Portugal from P-wave tele-seismic receiver functions. *Pure Appl. Geophys.* DOI 10.1007/s00024-016-1257-4.
- Duque, M.R., Mendes Victor, L., 1993. Heat flow and deep temperatures in South Portugal. *Studia Geophysica et Geodaetica*, 37, 279-292. <https://doi.org/10.1007/bf01624601>.
- Duque, M.R. 2016. Lithosphere Thickness, Heat Flow and Moho Depth in The South of Portugal. 2016 IOP Conf. Ser: Earth Environ. Sci., 44, 042016. DOI:10.1088/1755-1315/44/4/042016.
- Duque, M.R. 2018a. Heat Flow, Geotherms, Density and Lithosphere Thickness in SW of Iberia (South of Portugal). *International Journal of Terrestrial Heat Flow and Applied Geothermics*, 1, P. 18-22. DOI:10.31214/ijthfa.
- Duque, M.R., 2018b. An attempt to obtain heat sources in the crust using non-conventional methods, *Geophysical Research Abstracts*, 20, EGU2018-9554.
- IGM, 1997. Map of Natural Gamma Radiation (in Portuguese) Sheet 4 –Beira Interior, scale 1:200 000.
- Online Geoid Calculator – Source Forge. <https://geographiclib.sourceforge.io/cgi-bin/GeoidEval> (last utilization in January 2020).
- Hurter, S., and Haenel, R., 2002. Atlas of Geothermal Resources in Europe, Office for Official Publications of the European Communities, Luxemburg.
- Lamas, R., Miranda, M., Pereira, A., Ferreira, N., Neves, L., 2015. Distribuição dos elementos radiogénicos nas rochas granitoides aflorantes na Zona Centro- Ibérica (Centro e Norte de Portugal). *Proceedings of X Congresso Ibérico de Geoquímica*, 173-176.
- Lamas, R., Miranda, M.M., Pereira, A., Neves, L., Ferreira, N., Rodrigues, N., 2017. 3-D distribution of the radioelements in the granitic rocks of Northern and Central Portugal and geothermal implications. *Journal of Iberian Geology*, DOI:10.1007/s41513-017-0001-y.
- LNEG, 2013. Carta Radiométrica de Portugal Continental, escala 1:500 000.
- Machadinho, A., Figueiredo, F., Pereira, A., 2018. Modelação gravimétrica e magnética de granitos na região centro de Portugal. 10º Simpósio de Meteorologia e Geofísica da APMG-XX Aniversário da APMG, Lisboa, 20 a 22 de Março de 2017, pp. 37-42.
- Mancilla, F., Diaz, J., 2015. High resolution Moho topography map beneath Iberia and Northern Morocco from receiver function analysis. *Tectonophysics*, 663, 203-211.
- Miranda, M., Lamas, R., Pereira, A., Ferreira, N., Neves, L., 2015. Potencial térmico das rochas granitoides aflorantes na Zona Centro-Ibérica (Centro e Norte de Portugal). *Proceedings, X Congresso Ibérico de Geoquímica*.
- Pereira, A., Neves, L., 2011. Potencial EGS/HDR da região Centro e Norte de Portugal. Livro de Homenagem ao Professor Manuel Maria Godinho “Modelação de Sistemas Geológicos”, Universidade de Coimbra, pp.303-315.
- Pollett, A., Hasterok, D., Raimondo, T., Halpin, J.A., Hand, M., Bendall, B., McLaren, S., 2019. Heat flow in Southern Australia and connections with East Antarctica. *Geochemistry, Geophysics, Geosystems*, 20. <https://doi.org/10.1029/2019GC008418>.
- Rimi, A., 1999. Mantle heat flow and geotherms for the main geologic domains in Morocco. *Int. J. Earth Sci.*, vol 88, 458-466.
- Rimi, A., Fernandez, M., Manar, A., Matsushima, J., Okubo, Y., Morel, J.L., Winckel, A., Zeyen, H., 2005. Geothermal anomalies and analysis of gravity, fracturing and magnetic features in Morocco. *Proceedings of the World Geothermal Congress*, Antalya, Turkey.
- Rockwell, T., Fonseca, J., Madden, C., Dawson, T., Owen, L.A., Vilanova, S., Figueiredo, P., 2009. Paleo-seismology of the Vilariça Segment of the Manteigas-Bragança Fault in Northeastern Portugal. In: Reicherter, K., Michetti, A. M., Silva, P.G. (eds) *Paleo-seismology: Historical and Prehistorical records of Earthquake Ground Effects for Seismic Hazard Assessment*. Geol. Soc. London, Special Publications, 316, 2337-258. Doi:10.1144/SP316.15.

Veludo, I., Dias, N., Fonseca, P.E., Matias, L., Carrilho, F., Haberland, C., Villaseñor, A. 2017. Crustal seismic structure beneath Portugal and Southern Galicia (Western Iberia) and the role of Variscan inheritance. *Tectonophysics*, 717, 645-664. <https://doi.org/10.1016/j.tecto.2017.08.018>.